Journal of Luminescence 130 (2010) 2281–2287

Contents lists available at ScienceDirect

Journal of Luminescence

journal homepage: www.elsevier.com/locate/jlumin

# The investigation of the interaction between oxybutynin hydrochloride and bovine serum albumin by spectroscopic methods

Xing-jia Guo [a,*], Kui Jing [b], Chuang Guo [a], Yu-chun Jiang [a], Jiang Tong [a], Xiao-wei Han [a]

[a] College of Chemistry, Liaoning University, Shenyang 110036, PR China
[b] Environment College, Liaoning University, Shenyang 110036, PR China

ARTICLE INFO

*Article history:*
Received 22 August 2009
Received in revised form
4 July 2010
Accepted 9 July 2010
Available online 14 July 2010

*Keywords:*
Oxybutynin hydrochloride
Bovine serum albumin
Fluorescence quenching
Displacement studies

ABSTRACT

The mutual interaction of oxybutynin hydrochloride (OB) with bovine serum albumin (BSA) was investigated by fluorescence, UV–vis absorption, circular dichroism (CD), and Fourier transform infrared (FT-IR) spectroscopies under simulative physiological conditions. The results of fluorescence titration revealed that OB could quench the intrinsic fluorescence of BSA by static quenching and there was a single class of binding sites on BSA for this drug. The thermodynamic parameters $\Delta H$, $\Delta S$, and $\Delta G$ calculated at different temperatures indicated that hydrogen bonds and van der Waals interactions were the dominant intermolecular forces in stabilizing the OB–BSA complexes. According to the theory of Förster's non-radiation energy transfer, the binding distance $r$ between OB and BSA was evaluated to be 3.27 nm. The displacement experiments confirmed that OB could bind to site I of BSA. The FT-IR and CD spectra showed that the binding of OB to BSA induced conformational changes in BSA.



## 1. Introduction

Oxybutynin hydrochloride (α-cyclohexyl-α-hydroxybenzeneacetic acid 4-(diethylamino)-2-butynyl ester hydrochloride, structure shown in Fig. 1) is a smooth muscle relaxant drug mainly used to treat a number of bladder instability disorders associated with abnormal nerve impulses to the bladder. In these cases, OB reduces bladder activity and relieves symptoms of urgency, frequency, dysuria, and urinary incontinence [1].

Serum albumins are the most abundant proteins in blood. They have many important physiological functions. For instance, they contribute to the osmotic blood pressure and are chiefly responsible for the maintenance of blood pH. But the most important physiological role of albumins involves the binding, transport, and delivery of numerous ligands, such as fatty acids, drugs, and metal ions, in the bloodstream to their target organs. Therefore, the investigation of such molecules with respect to albumin binding is imperative of and fundamental importance.

Studies on the binding of drugs to albumins may provide information of structural features, which determine the therapeutic effectivity of drugs, and has become an important research field in life sciences, chemistry, and clinical medicine [2–6].

Bovine and human serum albumins display approximately 76% sequence homology, and the 3D structure of BSA is believed to be similar to that of HSA [7]. So the results of all the studies are consistent with the fact that bovine and human serum albumins are homologous proteins. Besides, because of BSA's medical importance, low cost, and ready availability, it is selected as our protein model in the present work.

BSA is composed of three linearly arranged, structurally homologous domains (I–III), and each domain in turn is the product of two sub-domains (A and B). BSA molecule has two tryptophan residues, which possess intrinsic fluorescence: Trp-134 in the first sub-domain IB of the albumin molecule and Trp-212 in sub-domain IIA. Trp-212 is located within a hydrophobic binding pocket of the protein and Trp-134 is located on the surface of the albumin molecule [8]. The binding sites of BSA for endogenous and exogenous ligands may be in these domains, and the principal regions of drugs binding sites of albumin are often located in hydrophobic cavities in sub-domains IIA and IIIA. The so called sites I and II are located in sub-domain IIA and IIIA of albumin, respectively. Many ligands bind specifically to serum albumin, for example, ketoprofen in site I [9], flufenamic acid, and ibuprofen in site II [10].

Spectroscopic techniques are often applied to reveal the accessibility of quenchers to albumin's fluorophore groups, help understand albumin's binding mechanisms to drugs, and provide clues on the nature of binding phenomenon [11].

In the present work, investigation on the interaction between OB and BSA is first reported using several spectroscopic techniques. The binding characteristics between OB and BSA were analyzed. The binding constants, the binding sites, and the binding distance along with thermodynamic parameters were estimated. In addition, the conformational changes of BSA were also explored.

* Corresponding author. Tel.: +86 24 62207809.
*E-mail address:* guoxja@sina.com (X.-j. Guo).

0022-2313/$ - see front matter © 2010 Elsevier B.V. All rights reserved.
doi:10.1016/j.jlumin.2010.07.005

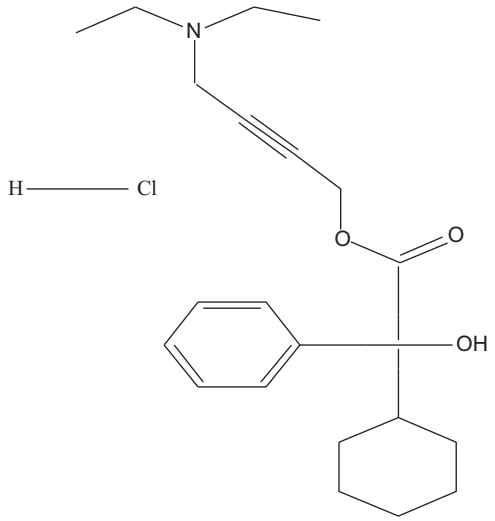


**Fig. 1.** Molecular structure of OB.

## 2. Experimental

### 2.1. Materials

The stock solutions of BSA (purity > 98%, purchased from Sino-American Biotechnology Company, China) and OB ( provided by Shenyang Watson Pharmaceutical Institute, China) were prepared by dissolving them in water. The stock solutions of ketoprofen and ibuprofen (obtained from the National Institute for Control Pharmaceutical and Products, China) were prepared by dissolving them in a small amount of ethanol, and diluting to the desired concentration with water. All working solutions were prepared in Tris–HCl buffer solution (0.01 M Tris, 0.10 M NaCl, pH 7.43). All other reagents were of analytical grade and doubly distilled water was used throughout.

### 2.2. Apparatus

Steady-state fluorescence measurements were carried out through a Cary Eclipse 300 FL spectrophotometer (Varian Company, USA) equipped with a thermostat bath and a 1.0 cm quartz cell; absorbance measurements were performed with a Cary 5000 UV–vis spectrophotometer (Varian Company, USA) equipped with a 1.0 cm quartz cell; CD measurements were performed with a JASCO–J–810 spectropolarimeter (JASCO, Japan) using a 0.1 cm quartz cell; FT-IR measurements were carried out with a Nicolet Nexus 670 FT-IR spectrometer (Thermo Nicolet Company, USA) equipped with a germanium attenuated total reflection (ATR) accessory, a deuterated triglycine sulphate (DTGS) detector, and a KBr beam splitter.

### 2.3. Spectroscopic measurements

All solutions were rested at least 10 min before the spectrum measurements. Appropriate blanks corresponding to the buffer were subtracted to correct the fluorescence or absorption background. The following quantitative analysis involved was carried out using the corrected fluorescence intensities at $\lambda_{em}=346$ nm at various temperatures.

#### 2.3.1. Fluorescence quenching spectra of BSA

Fluorescence measurements were carried out keeping the concentration of BSA fixed at $1.0\times10^{-5}$ mol $L^{-1}$ and that of OB varied from 0 to $8.0\times10^{-5}$ mol $L^{-1}$. The excitation wavelength was 280 nm and the intrinsic fluorescence emission spectra of BSA were recorded between 300 and 500 nm at three different temperatures (291, 298, and 310 K). The synchronous fluorescence spectra were scanned from 230 to 350 nm at $\Delta\lambda=15$ and 60 nm, respectively.

#### 2.3.2. UV–vis absorption spectra

The absorption spectra of BSA in the presence of different concentrations of OB were recorded in the range 200–500 nm at room temperature. BSA concentration was kept at $1.0\times10^{-5}$ mol $L^{-1}$ , while that of OB was varied from 0 to $13.3\times10^{-5}$ mol $L^{-1}$.

#### 2.3.3. FT-IR spectra

All FT-IR spectra were obtained via the attenuated total reflection (ATR) method with a resolution of 4 $cm^{-1}$ and 60 scans at room temperature. The background (containing all system components except protein) was collected at the same condition and subtracted from the spectra of sample solution to obtain the FT-IR spectra of protein. The subtraction criterion was that the original spectrum of protein solution between 2200 and 1800 $cm^{-1}$ was featureless [12].

#### 2.3.4. CD spectra

The CD spectra of BSA in the presence of OB were recorded in the wavelength range 190–250 nm at 0.1 nm intervals under constant nitrogen flush at room temperature. The concentration of BSA was kept at $2.0\times10^{-6}$ mol $L^{-1}$ and the molar ratio of OB to BSA was varied as 0:1, 10:1, and 20:1. Each CD spectrum was the average of three scans and the contributions of appropriate blanks corresponding to the buffer running under the same conditions were subtracted.

#### 2.3.5. Displacement experiments

The displacement experiments were performed using two site probes viz., ibuprofen and ketoprofen by keeping the concentrations of BSA and OB constant. The ratio of OB to BSA in the OB+BSA mixture solution was kept at 5:1 in order to keep non-specific binding of probes to a minimum. Then the fluorescence spectra of this mixture solution in the presence of ibuprofen and ketoprofen were recorded in the range 300–500 nm on excitation at 280 nm.

## 3. Results and discussion

### 3.1. Analysis of fluorescence quenching of BSA by OB

At the excitation wavelength of 280 nm, the fluorescence emission spectra of BSA with varying concentrations of OB are shown in Fig. 2. On increasing the concentration of OB, fluorescence of BSA regularly decreased and no distinct shift of the emission maximum wavelength was observed, indicating that OB interacted with BSA and quenched its intrinsic fluorescence, but the microenvironment around the chromophore of BSA was unchanged.

Fluorescence quenching is the decrease of the quantum yield of fluorescence by a fluorophore induced by a variety of molecular interactions with quencher molecule. Under the conditions of fixed pH, temperature, and ionic strength, fluorescence quenching may result from ground complex formation, energy transfer, and dynamic quenching processes [13].

Dynamic quenching refers to a process where the fluorophore and the quencher come into contact during the lifetime of the excited state, whereas static quenching refers to fluorophore–quencher complex formation.

In order to predict the possible quenching mechanism of drugs binding to serum albumin, the fluorescence quenching data are usually analyzed by the Stern–Volmer equation [14]

$$\frac{F_0}{F} = 1 + K_{SV}[Q] \quad (1)$$

where $F_0$ and $F$ are the fluorescence intensities in the absence and presence of quencher, respectively. [$Q$] is the concentration of quencher and $K_{sv}$ the Stern–Volmer quenching constant.

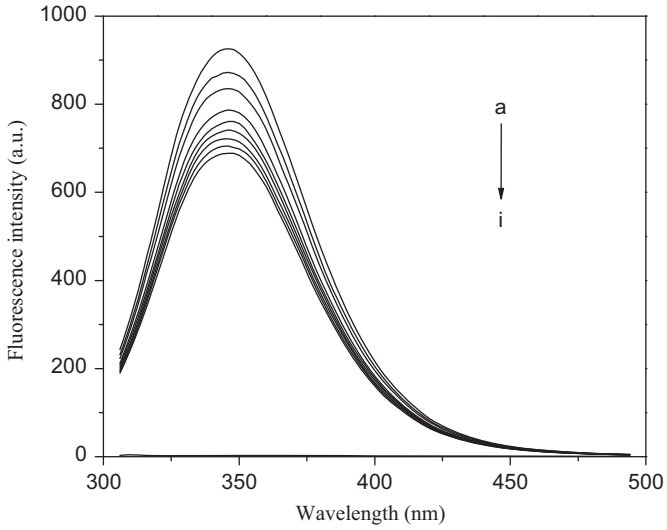


**Fig. 2.** Fluorescence emission spectra of BSA in the presence of different concentrations of OB (pH=7.43, $T$=291 K, $\lambda_{ex}$=280 nm): $c$(BSA)=$1.0\times10^{-5}$ mol $L^{-1}$; $c$(OB)/($\times10^{-5}$), a→i, from 0.0 to 8.0 mol $L^{-1}$ at increments of 1.0 mol $L^{-1}$.

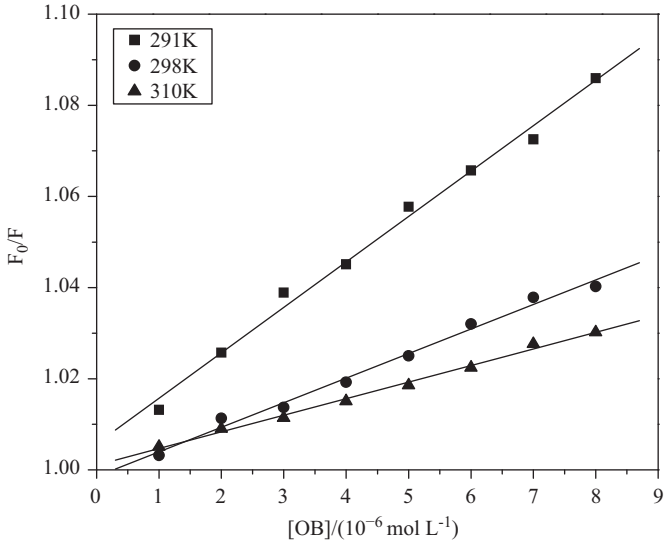


**Fig. 3.** Stern–Volmer plots for the quenching of BSA by OB at three different temperatures.

Accord to the measured fluorescence intensities, Eq. (1) was applied to determine $K_{SV}$ by a linear regression of the plot of $F_0/F$ against [$Q$] (Fig. 3) at different temperatures. The results are listed in Table 1. Fig. 3 shows that each plot exhibits a good linear relationship and the slope of the Stern–Volmer plot decreases with rising temperature, which suggests that the possible quenching mechanism is not initiated by dynamic collision but from the formation of a complex.

### 3.2. UV–vis absorption spectra

UV–vis absorption measurement is a very simple method and applicable to explore the structural change and know the complex formation [15]. The absorption spectra of BSA in the presence and absence of OB were recorded and are shown in Fig. 4. It is clear from this figure that the absorbance peak around 278 nm decreased with the addition of OB, indicating that OB could bind to BSA to form the OB–BSA complexes. Therefore, the result of BSA absorption spectra reconfirms that the mechanism of intrinsic fluorescence quenching of BSA is a static quenching process.

### 3.3. Binding constants and binding sites

When small molecules bind independently to a set of equivalent sites on a macromolecule, the equilibrium between free and bound molecules is given by the following equation [16]:

$$\log\left(\frac{F_0 - F}{F}\right) = \log K_a + n\log[Q] \quad (2)$$

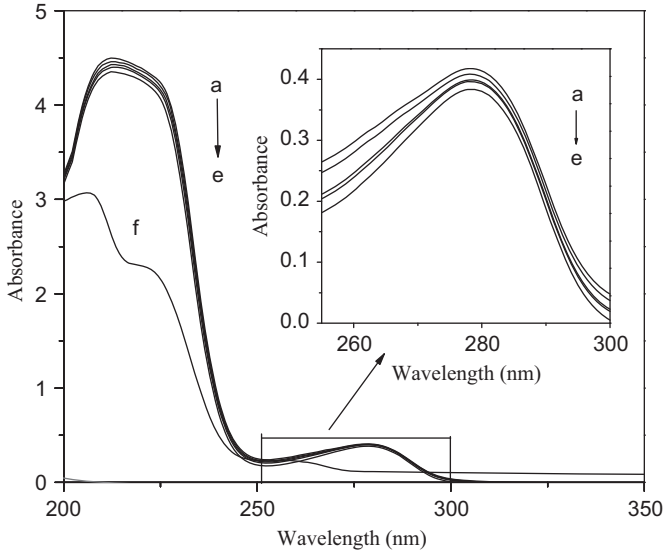


**Fig. 4.** Absorption spectra of BSA in the presence of OB. $c$(BSA)=$1.0\times10^{-5}$ mol $L^{-1}$; $c$(OB)/($\times10^{-5}$), a→e, from 0.0 to 13.3 mol $L^{-1}$ at increments of 3.3 mol $L^{-1}$; and (f) A concentration of $13.3\times10^{-5}$ mol $L^{-1}$ OB only.

**Table 1**
The Stern–Volmer quenching constants and thermodynamic parameters of OB–BSA system at different temperatures.

| pH | $T$ (K) | $K_{sv}$ ($10^3$ L mol$^{-1}$) | $R^a$ | $\Delta H$ (kJ mol$^{-1}$) | $\Delta S$ (J mol$^{-1}$ K$^{-1}$) | $\Delta G$ (kJ mol$^{-1}$) |
|---|---|---|---|---|---|---|
| 7.43 | 291 | 9.965 | 0.9963 | −38.38 | −56.11 | −22.05 |
| | 298 | 5.389 | 0.9950 | | | −21.66 |
| | 310 | 3.639 | 0.9972 | | | −20.99 |

[a] $R$—Linear correlation coefficient.

where in the present case, $K_a$ and $n$ are the binding constant and the number of binding sites, respectively.

The values of $K_a$ and $n$ were obtained from the intercept and slope of the plots of $\log((F_0-F)/F)$ versus $\log[OB]$ (not shown), respectively, and are listed in Table 2. The values of $K_a$ decrease slightly with the rising temperature, but $n$ is approximately equal to 1, indicating that OB and BSA formed the mol ratio 1:1 complex and the complex would be partly decomposed with rising temperature.

### 3.4. Thermodynamic parameters and nature of the binding forces

The interaction forces between a small molecule and biomolecule mainly include hydrophobic force, electrostatic interactions, Van der Waals interactions, hydrogen bonds, etc. In order to further elucidate the interaction of OB with BSA, the thermodynamic parameters were calculated. If the enthalpy change ($\Delta H$) does not vary significantly over the temperature range studied, then its value and that of $\Delta S$ can be determined from the van't Hoff equation

$$\ln K = -\frac{\Delta H}{RT} + \frac{\Delta S}{R} \tag{3}$$

where $\Delta S$ is the entropy change; constant $K$ is analogous to the Stern–Volmer quenching constant $K_{SV}$ at the corresponding temperature [17]; and $R$ is the gas constant.

In the OB–BSA system, the enthalpy change ($\Delta H$) and the entropy change ($\Delta S$) were obtained from the slope and intercept of the fitted curve of $\ln K_{sv}$ against $1/T$ (Fig. 5), respectively. Then the free energy change ($\Delta G$) was estimated from the following relationship: $\Delta G = \Delta H - T\Delta S$. The values of these thermodynamic parameters were listed in Table 1. The negative values of $\Delta G$, $\Delta S$, and $\Delta H$ mean that the binding process is spontaneous and mainly driven by enthalpy, whereas entropy is unfavorable for it. Moreover, according to the rules summarized by Ross and Subramanian [18], the negative values of $\Delta S$ and $\Delta H$ suggest that hydrogen bonds and van der Waals interactions played major roles in the binding process and contributed to the stability of the OB–BSA complex.

**Table 2**
Binding constants $K_a$ and binding sites $n$ at different temperatures for the OB–BSA system

| $T$ (K) | $K_a$ ($10^3$ L mol$^{-1}$) | $n$ | $R^a$ |
|---|---|---|---|
| 291 | 8.594 | 1.0784 | 0.9937 |
| 298 | 2.637 | 0.9577 | 0.9966 |
| 310 | 2.131 | 0.9391 | 0.9861 |

[a] $R$—Linear correlation coefficient.

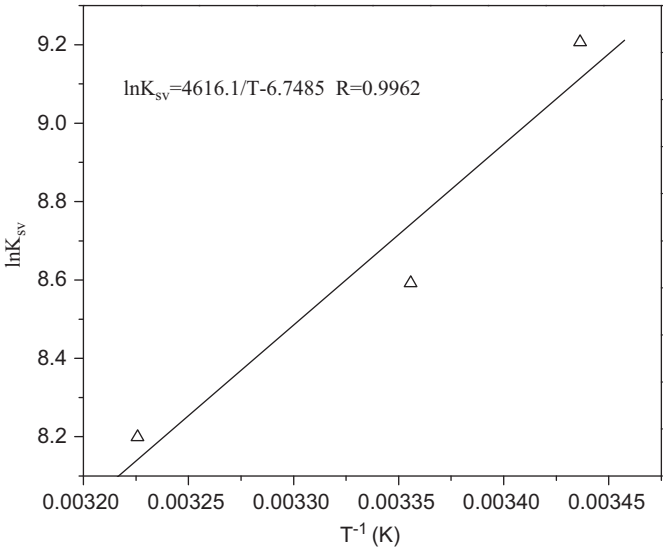


**Fig. 5.** The van't Hoff plot for the interaction of BSA and OB.

### 3.5. Energy transfer from BSA to OB

Fluorescence resonance energy transfer (FRET) has been used as a "spectroscopic ruler" for measuring molecular distances in biological and macromolecular systems. According to the theory of Förster's non-radiation energy transfer [19], the efficiency of energy transfer mainly depends on the following factors: (1) the donor can produce fluorescence, (2) fluorescence emission spectrum of the donor and UV–vis absorbance spectrum of the acceptor have more overlap, and (3) the distance between the donor and the acceptor is less than 8 nm.

The efficiency of energy transfer between the donor and acceptor, $E$, can be calculated by the following equation [16]:

$$E = 1 - \frac{F}{F_0} = \frac{R_0^6}{(R_0^6 + r^6)} \tag{4}$$

where $E$ denotes the efficiency of energy transfer between the donor and the acceptor and $R_0$ is the critical distance where the efficiency of energy transfer is 50%. The value of $R_0^6$ can be calculated using the equation:

$$R_0^6 = 8.8 \times 10^{-25}\,(JK^2\varphi n^{-4}) \tag{5}$$

where $K^2$ is the spatial orientation factor related to the geometry of the donor and acceptor of dipoles, and $K^2=2/3$ for random orientation as in fluid solutions; $n$ is the averaged refracted index of the medium in the wavelength range where spectral overlap is significant; $\varphi$ is the fluorescence quantum yield of the donor; and $J$ the spectral overlap integral between the fluorescence emission spectrum of the donor and the absorption spectrum of the acceptor. The value of $J$ can be calculated by the equation

$$J = \frac{\int_0^\infty F(\lambda)\varepsilon(\lambda)\lambda^4\,d\lambda}{\int_0^\infty F(\lambda)d\lambda} \tag{6}$$

where $F(\lambda)$ is the corrected fluorescence intensity of the donor in the wavelength range $\lambda$–$\lambda+\Delta\lambda$ and $\varepsilon(\lambda)$ is the molar absorption coefficient of the acceptor at wavelength $\lambda$.

The overlap of the UV–vis absorption spectrum of OB with the fluorescence emission spectrum of BSA is shown in Fig. 6.

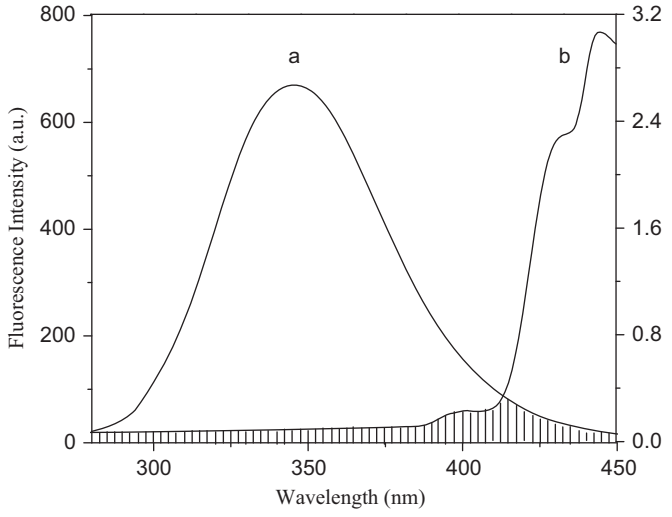


**Fig. 6.** Overlap of the fluorescence spectrum of BSA (a) and the absorbance spectrum of OB (b) ($c$(BSA)/$c$(OB)=1:1).

In the present case, $n=1.36$ and $\varphi=0.15$ [2]. From Eqs. (4)–(6), $J=1.937\times10^{-14}$ cm$^3$ L mol$^{-1}$, $E=0.26$, $R_0=2.74$, and $r=3.27$ nm were calculated. The binding distance $r=3.27$ nm is less than 8 nm, indicating that the energy transfer from BSA to OB occured with high possibility [20].

### 3.6. Displacement experiments of site probes

BSA has a large hydrophobic cavity that can accommodate two or more ligands. When two ligands (denoted by $L_1$ and $L_2$ ) bind to BSA simultaneously, two types of interaction can occur [21]:

1. competitive binding

$$L_1 \xrightarrow{+BSA} L_1\text{–BSA} \xrightarrow{+L_2} L_2\text{–BSA}+L_1$$

2. non-competitive binding

$$L_1 \xrightarrow{+BSA} L_1\text{–BSA} \xrightarrow{+L_2} L_2+\text{BSA}\text{–}L_1$$

In order to identify the location of the OB binding site on BSA, the displacement experiments were carried out using the site probes ibuprofen and ketoprofen. The percentage of fluorescence probe displaced by the drug was determined by measuring the changes in fluorescence intensity according to the method proposed by Sudlow et al. [22]:

$$F_2/F_1\times100\% \tag{7}$$

where $F_1$ and $F_2$ denote the fluorescence of drug plus protein without the probe and with the probe, respectively.

According to the spectral data measured in the displacement experiments, the plots of $F_2/F_1$ against site probe concentration were obtained and are shown in Fig. 7. It can be seen from Fig. 7 that the fluorescence was remarkably affected by adding ketoprofen, and conversely the addition of ibuprofen to the same solution. These results indicated that ketoprofen displaced OB from the binding site while ibuprofen had a little effect on the binding of OB to BSA. Hence, it can be concluded that OB was bound to site I in subdomain IIA of BSA.

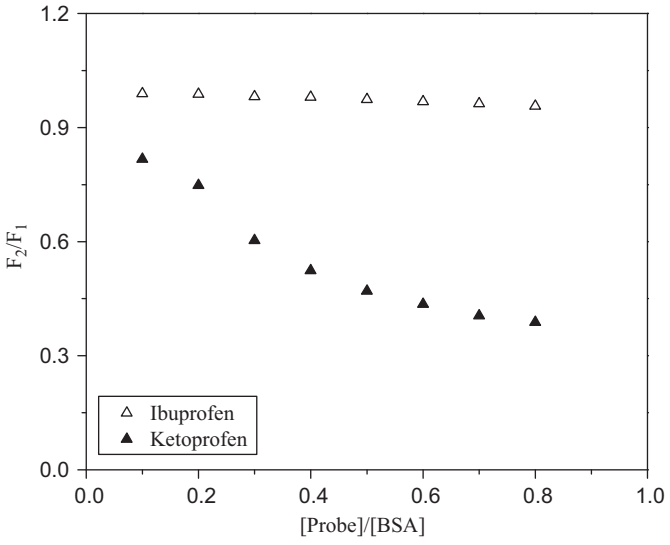


**Fig. 7.** Effect of site marker probes on the fluorescence OB–BSA; $c$(BSA)$=1.0\times10^{-5}$ mol L$^{-1}$.

### 3.7. FT-IR spectra

Infrared spectra of proteins exhibit a number of amide bands, which represent different vibrations of peptide moieties. Among the amide bands of the protein, amide I band (mainly C=O stretch) and amide II band (C–N stretch coupled with N–H bending mode) have been widely used as the typical ones. They both have relationship with the secondary structure of the protein. However, the amide I band is more sensitive to the change of protein secondary structure than that of amide II [23].

To explore the changes of BSA secondary structure after OB was bound to BSA, the FT-IR spectra of BSA were recorded. The FT-IR spectra and difference spectra of BSA (Fig. 8) showed an obvious shift of the amide I band from 1652.7 to 1648.9 cm$^{-1}$ and a decrease in intensity. These changes indicated that the secondary structure of BSA was changed. From the molecular structure of OB and the nature of the binding forces, it can be deduced that the O–H···O hydrogen bonds may be formed between O–H group in OB and oxygen atoms of the aromatic amino acid residues in BSA, which induced the rearrangement of the polypeptide carbonyl hydrogen bonding network. Consequently the content of the α-helical structure in BSA was changed.

### 3.8. CD spectra

To further investigate whether any conformational changes of BSA molecules occurred in the binding reaction, the CD spectra of BSA were measured in the absence and presence of OB, and shown in Fig. 9. These spectra exhibited two negative bands at 208 and 222 nm, characteristic of a predominantly α-helical structure of BSA [24]. With the increase in OB concentration, band intensity of curves (a→c) decreased regularly. Moreover, the CD spectra of BSA in the absence and the presence of OB are similar in shape, indicating that the structure of BSA after the addition of OB is also predominantly α-helix.

The CD results were expressed in terms of mean residue ellipticity (*MRE*) in deg cm$^2$ dmol$^{-1}$ according to the following equation [25]:

$$MRE=\frac{observedCD(medg)}{C_p nl\times10} \tag{8}$$

where $C_p$ is the molar concentration of the protein, $n$ the number of amino acid residues, and $l$ the path length. The α-helical contents of

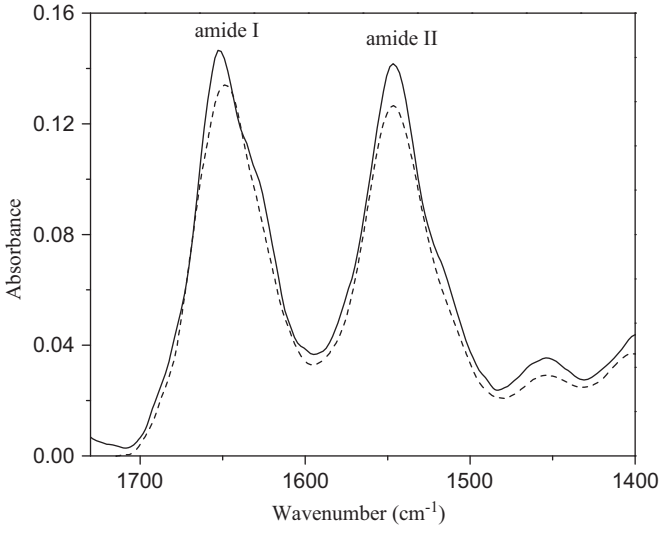


**Fig. 8.** FT-IR spectra of free BSA (solid line) and difference spectra of OB+BSA[(OB+BSA solution)−(OB solution)] (dash line) in the region of 1730−1400 cm$^{-1}$; $c$(OB)$=5.4\times10^{-3}$; $c$(BSA)$=5\times10^{-4}$ mol L$^{-1}$.

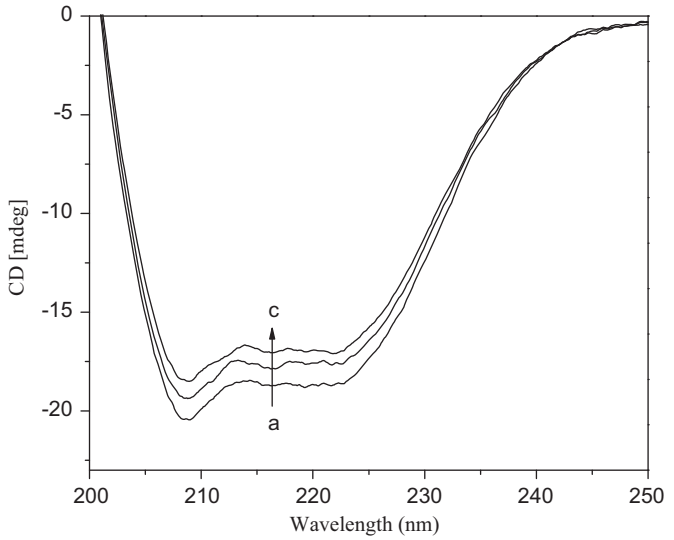


**Fig. 9.** Circular dichroism spectra of BSA−OB system at pH=7.43. Concentration ratios of OB to BSA are 0:1, 10:1, and 20:1 (from curve a to c).

free and combined BSA were calculated from MRE values at 208 nm using the equation [25]

$$\alpha\text{-}Helical\ (\%) = \frac{-MRE_{208} - 4000}{33{,}000 - 40{,}000} \times 100 \quad (9)$$

where $MRE_{208}$ is the observed *MRE* value at 208 nm, 4000 is the *MRE* of the β-form and random coil conformation cross at 208 nm and 33,000 is the *MRE* value of a pure α-helix at 208 nm.

From Eqs. (8) and (9), the α-helix contents in the secondary structure of BSA were calculated to be 46.4% in free BSA and 43.2% and 40.7% at molar ratios of OB to BSA 10:1 and 20:1, respectively. A small decrease of α-helix percentage indicated that OB bound with the amino acid residues of the main polypeptide chain of protein and the hydrogen bonding networks of the protein was destroyed [26]; consequently the binding of OB to BSA induced slight unfolding of the constitutive polypeptides of protein.

### 3.9. Synchronous fluorescence spectra

The synchronous fluorescence spectra can give information about the molecular environment in a vicinity of the chromophore molecules. Synchronous fluorescence of BSA can be used to study the environment of amino acid residues by measuring the possible shift in wavelength emission maximum, the shift in the position of emission maximum corresponding to changes of polarity around the chromophore molecule [27]. When the difference between excitation wavelength and emission wavelength is set at 15 or 60 nm, synchronous fluorescence gives the characteristic information of tyrosine or tryptophan residues [28]. The effects of OB on BSA synchronous fluorescence are shown in Fig. 10. It is apparent from Fig. 10 that no significant shift in the maximum emission wavelength was observed when $\Delta\lambda=15$ or 60 nm with the addition of OB, indicating that polarities around the tyrosine and tryptophan residues have not been changed. So the microenvironments around the tryptophan and tyrosine residues have no discernable change during the binding.

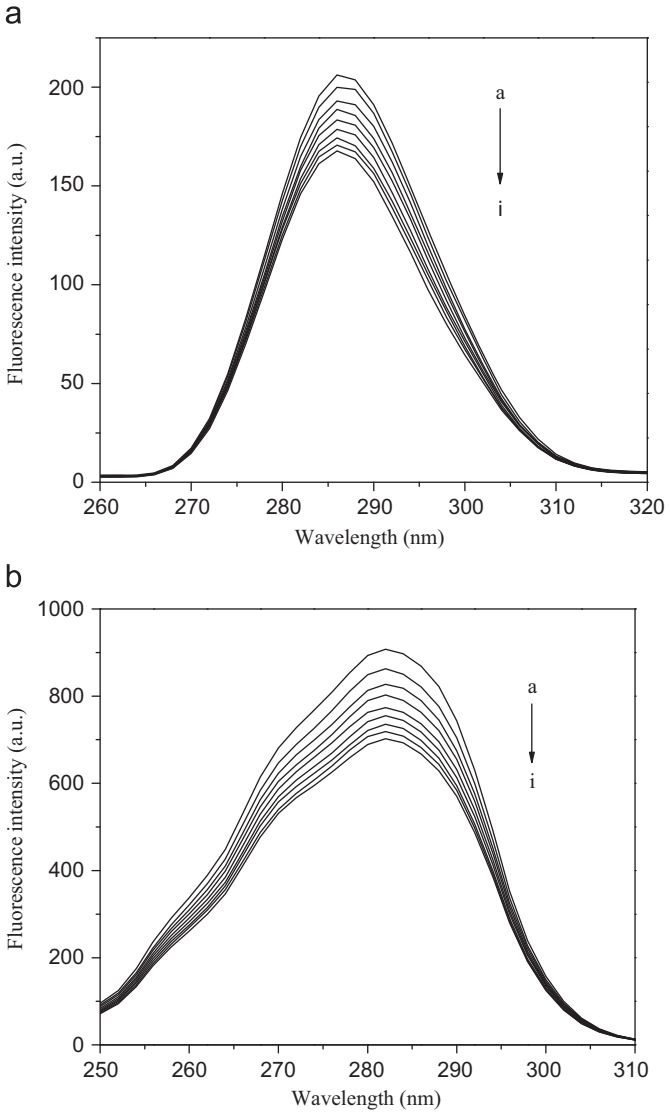


**Fig. 10.** Synchronous fluorescence spectra of BSA. (a) $\Delta\lambda=15$; (b) $\Delta\lambda=60$ nm; c(BSA)$=1.0\times10^{-5}$ mol L$^{-1}$; $c$(OB)/($\times10^{-5}$), a→i, from 0.0 to 8.0 mol L$^{-1}$ at increments of 1.0 mol L$^{-1}$.

## 4. Conclusions

In this paper, the interaction of OB with BSA has been investigated by several spectroscopic techniques. The fluorescence quenching results showed that the intrinsic fluorescence of BSA was quenched through a static quenching process. Hydrogen bonds and van der Waals interactions played major roles in stabilizing the OB–BSA complexes. The distance $r$ between OB and BSA obtained indicated that energy transfer from BSA to OB occurred. Displacement experiments demonstrated that the binding of OB to BSA primarily took place in sub-domain IIA, so Trp-212 is near or within the OB binding site. The results of CD and FT-IR spectra showed that the formation of OB–BSA complexes induced changes in the protein secondary structure with a slight reduction in the α-helix content.

The binding study of drugs with protein is of great importance in pharmacy, pharmacology, and biochemistry. This study will not only help understand the transportation and distribution of OB in blood but also elucidate the mechanism.

## Acknowledgement

We gratefully acknowledge financial support of the Education Foundation of Liaoning Province, China (Grant no. 20060362).

## References


[1] M.J. O'Neil, A. Smith, P.E. Heckelman, in: The Merck Index, An Encyclopedia of Chemicals, Drugs and Biologicals, 13th ed., Merck, Inc., Whitehouse Station, NJ, USA, 2001 p. 1245.
[2] P.B. Kandagal, S. Ashoka, J. Seetharmappa, J. Pharm. Biomed. 41 (2006) 393.
[3] Z.J. Cheng, Y.T. Zhang, J. Mol. Struct. 889 (2008) 20.
[4] Y.N. Ni, G.L. Liu, S. Kokot, Talanta 76 (2008) 513.
[5] A.R. Timerbaev, C.G. Hartinger, S.S. Aleksenko, Chem. Rev. 106 (2006) 2224.
[6] P.L. Gentili, F. Ortica, G. Favaro, J. Phys. Chem. B 112 (2008) 16793.
[7] C. Leslie, C.J.W. Scott, F.I. Cair, Med. Lab. Sci. 49 (1992) 319.
[8] S.Z. Hao, S.D. Liu, X.H. Wang, X.J. Cui, L.P. Guo, J. Lumin. 129 (2009) 1320.
[9] X.M. He, D.C. Carter, Nature 358 (1992) 209.
[10] I. Sjoholm, B. Ekman, A. Kober, I. Ljungstedt–Pahlman, B. Seiving, T. Sjodin, Mol. Pharmacol. 16 (1979) 767.
[11] N. Wang, L. Ye, F.F. Yan, R. Xu, Int. J. Pharm. 351 (2008) 55.
[12] A.C. Dong, P. Huang, W.S. Caughey, Biochemistry 29 (1990) 3303.
[13] M. Bhattacharyya, U. Chaudhuri, R.K. Poddar, Biochem. Biophys. Res. Commun. 167 (1990) 1146.
[14] J.R. Lakowicz, in: Principles of Fluorescence Spectroscopy, 2nd ed., Plenum Press, New York, 1999 p. 237.
[15] S. Ashoka, J. Seetharamappa, P.B. Kandagal, S.M.T. Shaikh, J. Lumin. 121 (2006) 179.
[16] C. Wang, Q.H. Wu, Z. Wang, J. Zhao, Anal. Sci. 22 (2006) 435.
[17] S.F. Sun, B. Zhou, H.N. Hou, Y. Liu, G.Y. Xiang, Int. J. Biol. Macromol. 39 (2006) 197.
[18] P.D. Ross, S. Subramanian, Biochemistry 20 (1981) 3096.
[19] T. Förster, Modern Quantum Chemistry, vol. 3, Academic Press, New York, 1965 p. 93.
[20] B. Valeur, J.C. Brochon, in: New Trends in Fluorescence Spectroscopy, 6th ed., Springer Press, Berlin, 1999 p. 25.
[21] Y.N. Ni, X. Zhang, S. Kokot, Spectrochim. Acta A 71 (2009) 1865.
[22] G. Sudlow, D.J. Birkett, D.N. Wade, Mol. Pharmacol. 12 (1976) 1052.
[23] K.S. Witold, H.M. Henry, C. Dennis, Biochem. 32 (1993) 389.
[24] M.S. Oh, K.S. Kim, Y.K. Jang, C.Y. Maeng, S.H. Min, M.H. Jang, S.O. Yoon, J.H. Kim, H.J. Hong, J. Immunol. Methods 283 (2003) 77.
[25] G. Hong, L. Liandi, L. Jiaqin, Q. Kong, C. Xingguo, Z. Hu, J. Photochem. Photobiol. Part A 167 (2004) 213.
[26] Y.Z. Zhang, J. Dai, X.P. Zhang, X. Yang, Y. Liu., J. Mol. Struct. 888 (2008) 152.
[27] B.F. Pan, F. Gao, L.M. Ao, J. Magn. Magn. Mater. 293 (2005) 252.
[28] E.A. Brustein, N.S. Vedenkina, M.N. Irkova, Photochem. Photobiol. 18 (1973) 263.